

Ramsey Interference in a Multi-level Quantum System

J. P. Lee,^{1,2} A. J. Bennett,^{1,*} J. Skiba-Szymanska,¹ D.

J. P. Ellis,¹ I. Farrer,³ D. A. Ritchie,³ and A. J. Shields¹

¹*Toshiba Research Europe Limited, Cambridge Research Laboratory,
208 Science Park, Milton Road, Cambridge, CB4 0GZ, U. K.*

²*Engineering Department, University of Cambridge,
9 J. J. Thomson Avenue, Cambridge, CB3 0FA, U. K.*

³*Cavendish Laboratory, Cambridge University,
J. J. Thomson Avenue, Cambridge, CB3 0HE, U. K.*

(Dated: July 31, 2018)

Abstract

We report Ramsey interference in the excitonic population of a negatively charged quantum dot revealing the coherence of the state in the limit where radiative decay is dominant. Our experiments show that the decay time of the Ramsey interference is limited by the spectral width of the transition. Applying a vertical magnetic field induces Zeeman split transitions that can be addressed by changing the laser detuning to reveal 2, 3 and 4 level system behaviour. We show that under finite field the phase-sensitive control of two optical pulses from a single laser can be used to prepare both population and spin qubits simultaneously.

*Electronic address: anthony.bennett@crl.toshiba.co.uk

Ramsey interferometry has found use in caesium atomic clocks and in investigations of the quantum nature of the electromagnetic field [1, 2]. Using this high precision technique to study zero dimensional defects in solid state systems promises new applications and insights [3–6]. Prior measurements of RI between exciton population levels in quantum dots (QDs) have used one of two techniques. In some works [3, 7, 8], the laser is resonant with a transition and measurement of the population is made in photocurrent, which necessitates the destruction of the excitation, shortening its lifetime. Alternatively, optical readout of the population has been made when excitation occurs via a phonon-assisted transition [7] or a two-photon transition [4] and thus the laser can be removed by spectral filtering.

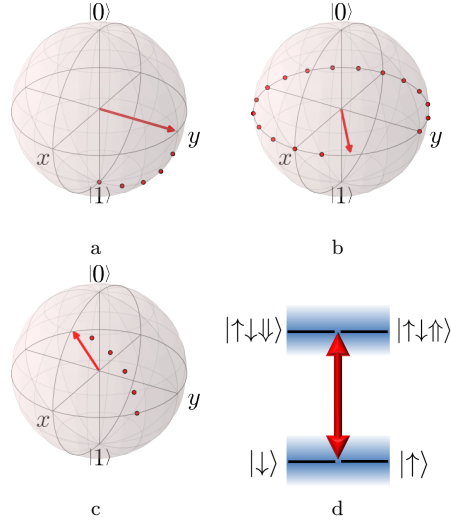


FIG. 1: **a)** A $\frac{\pi}{2}$ pulse creates a coherent superposition of the excited and ground states; the Bloch vector is rotated by $\frac{\pi}{2}$ about the x-axis. **b)** The system undergoes free evolution; the Bloch vector precesses about the z-axis. **c)** A second $\frac{\pi}{2}$ pulse maps the system into the excited or ground state dependent on the phase difference between the pulses; the Bloch vector is rotated by $\frac{\pi}{2}$ about the x-axis. **d)** In zero magnetic field the negatively charged QD behaves as a two level system. (Bloch spheres were produced with [10]).

Here we demonstrate a direct measurement of RI in the resonant fluorescence (RF) of a QD, building on the recent demonstration of pulsed RF [9]. The measurements are performed on the negative trion transition and dependent on the external magnetic field and laser energy, we observe 2, 3 and 4 level system behaviour. This leads to a rich variety of interferograms with exponential decays, beats and oscillations which reveal information about

the coherence of the exciton and the trapped charge. Our results show how a single laser can be used to prepare a population qubit simultaneously with a spin qubit, opening new possibilities to control and measure the dynamics of spin-qubits in mesoscopic semiconductor systems.

Ramsey interference (RI) fringes are the result of the oscillation in the population of a state of as a function of the phase difference between two $\frac{\pi}{2}$ pulses. The first pulse creates a superposition between the ground and excited state - interpreted as a $\frac{\pi}{2}$ rotation of the Bloch vector about the x-axis of the Bloch sphere (Figure 1a). The system then undergoes free evolution - the Bloch vector precesses about the equator of the Bloch sphere (Figure 1b) at a frequency determined by the energy difference between the ground and excited states. The second $\frac{\pi}{2}$ pulse then maps then the system to the ground or excited state dependent on the phase difference of the two pulses. Again, this is interpreted as a rotation of the Bloch vector about the x-axis (Figure 1c). At zero magnetic field the energy levels of a negatively charged QD are spin independent, so the dot behaves as a two level system (Figure 1d).

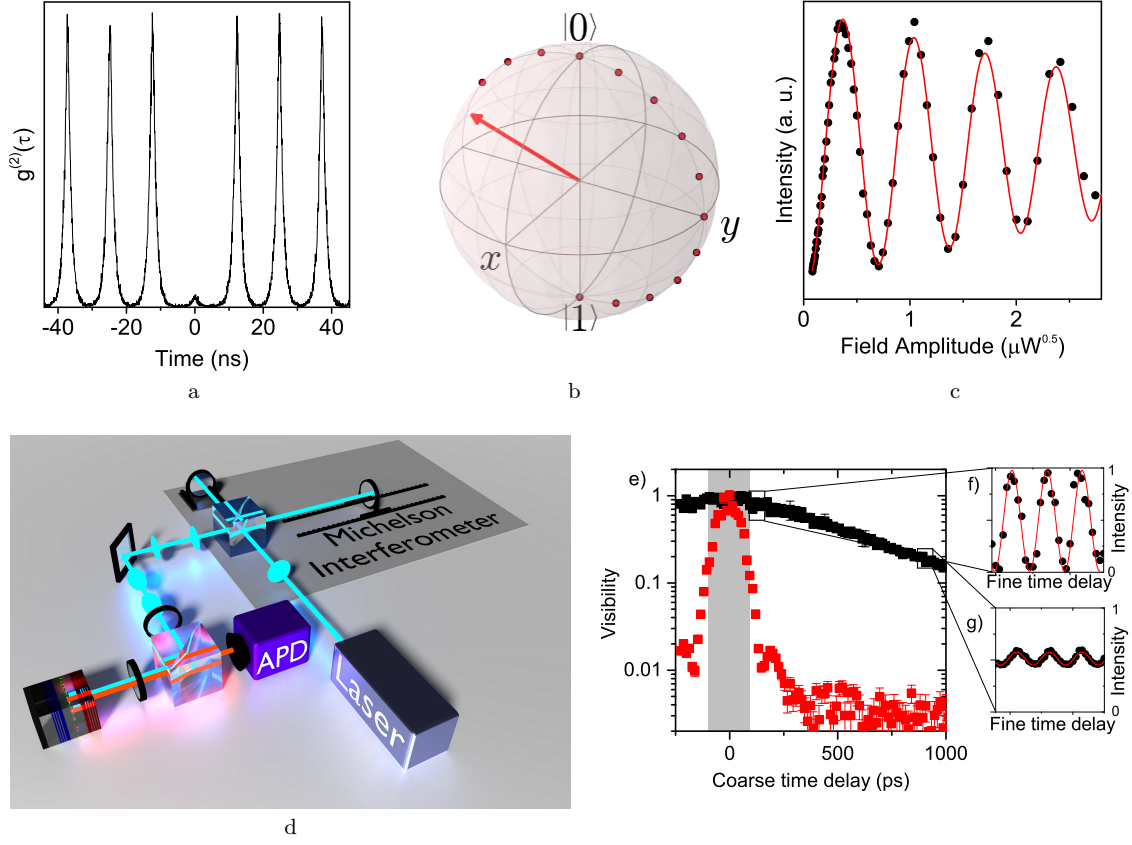


FIG. 2: **a)** A pulsed Hanbury-Brown and Twiss $g^{(2)}(\tau)$ measurement using 0.7π -pulses. The absence of a peak at $\tau = 0$ is indicative of a single photon source. **b)** The rotation of the Bloch vector about the x-axis. **c)** The emitted light intensity as a function of the square root of pulse power shows several Rabi oscillations. **d)** An illustration of our experimental setup for performing RI. Two pulses with a variable separation are created by a Michelson interferometer and directed to the QD-Light Emitting Diode (QD-LED) via a Polarising Beam Splitter (PBS) and a $\frac{\lambda}{4}$ -waveplate. Light from the QD-LED is polarisation filtered by the PBS and collected by an avalanche photodiode. **e)** (Red) Power measured in front of the sample. (Black) The visibility of the Ramsey fringes as a function pulse separation. The grey area of the graph indicates the range of pulse separations over which there is a significant overlap between the input laser pulses. **f)** A sinusoidal oscillation in emission intensity as a function of fine time delay at a short pulse separation. **g)** A sinusoidal oscillation in the emission intensity as a function of fine time delay at a longer pulse separation.

The InGaAs dot used was embedded in the undoped region of an LED planar microcavity

cooled to 5K. The device was held below the threshold voltage so no electroluminescence was seen, but the dot was loaded with an electron. Excitation was performed by pulsed RF with 57 ps pulses, which are short relative to the exciton lifetime (955 ± 1 ps). Cross-polarisation filtering was used to separate the excitation light from the emitted light and the emitted light was not spectrally filtered. This ensured that the spectral density function of the emitted photons remained intact, preventing an artificial increase in the decay time of the Ramsey fringe visibility. To determine that we are exciting a single quantum emitter we perform a Hanbury-Brown and Twiss measurement and record $g^{(2)}(0) = 0.06$ (Figure 2a).

Next, we demonstrate that we can coherently manipulate the excitation population by rotating the Bloch vector about the x-axis (Figure 2b). We do this by recording the emitted light intensity as a function of the square root of pulse power and observing Rabi oscillations with some damping [11–13] (Figure 2c).

We use the setup illustrated in Figure 2d to apply the Ramsey pulse sequence and record the emitted light intensity as a function of pulse separation. Scanning the position of the moveable mirror of the Michelson interferometer allows us to control the pulse separation and to record the emitted light intensity after polarisation filtering using a silicon avalanche-photodiode. We observe a sinusoidal variation in the emission intensity (Figures 2f and 2g) from which we can extract the visibility at each pulse separation time (2e in black). The visibility decays exponentially with a decay time of 510 ± 10 ps. The decay time is close to the coherence time inferred from a linewidth measurement (600 ± 20 ps), as expected from the Wiener-Khinchin Theorem ([14]). Figure 2e also shows the interference between the laser pulses measured in front of the sample (red). Due to this effect, oscillations shown in the grey region cannot be ascribed to RI. Outside of this region the low noise floor indicates that the oscillations are a result of RI.

Applying a magnetic field in the Faraday geometry removes the degeneracy between the spin-up and spin-down states resulting in 4-levels with distinct energies (Figure 3a). There are now two transitions allowed by the selection rules with an energy difference consistent with a combined electron and hole g-factor of $|g_e + g_h| = 2.88 \pm 0.03$. We set the laser energy between the two transition energies in order to excite both transitions equally (Figure 3 c).

Here we observe RI with the same decay time as at zero field (illustrated as a grey line in Fig. 3b), but with a beating pattern in the interference fringes (Figure 3b). The beat frequency corresponds to the energy difference between the allowed transitions. These results

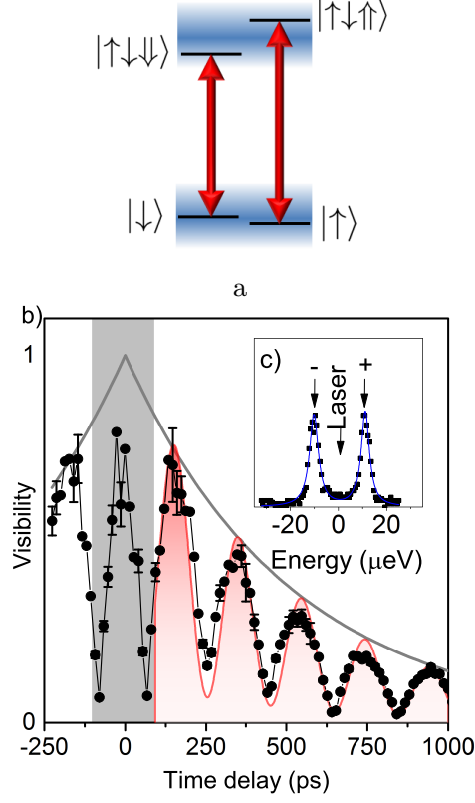


FIG. 3: **a)** In a Faraday magnetic field there are two allowed transitions. **b)** A beating in the Ramsey fringe visibility at 125 mT corresponding to the energy difference between the two allowed transitions is seen inside an exponentially decaying envelope. The grey area indicates the region of overlap between the input pulses and the grey exponential decay is a fit to the decay envelope of the 2-level system as in Figure 2e. **c)** The energy of the excitation laser is tuned to excite both allowed transitions.

are explained by considering two independent 2-level systems and can be represented as a Bloch sphere with two Bloch vectors. The two vectors precess about the z-axis at different rates and move in and out of phase with each other. When they are in phase we see a peak in visibility and when they are out of phase we see a minimum. The beat visibility does not decay faster than the exponentially decaying envelope, suggesting that the two transitions retain mutual coherence on a timescale longer than several nanoseconds.

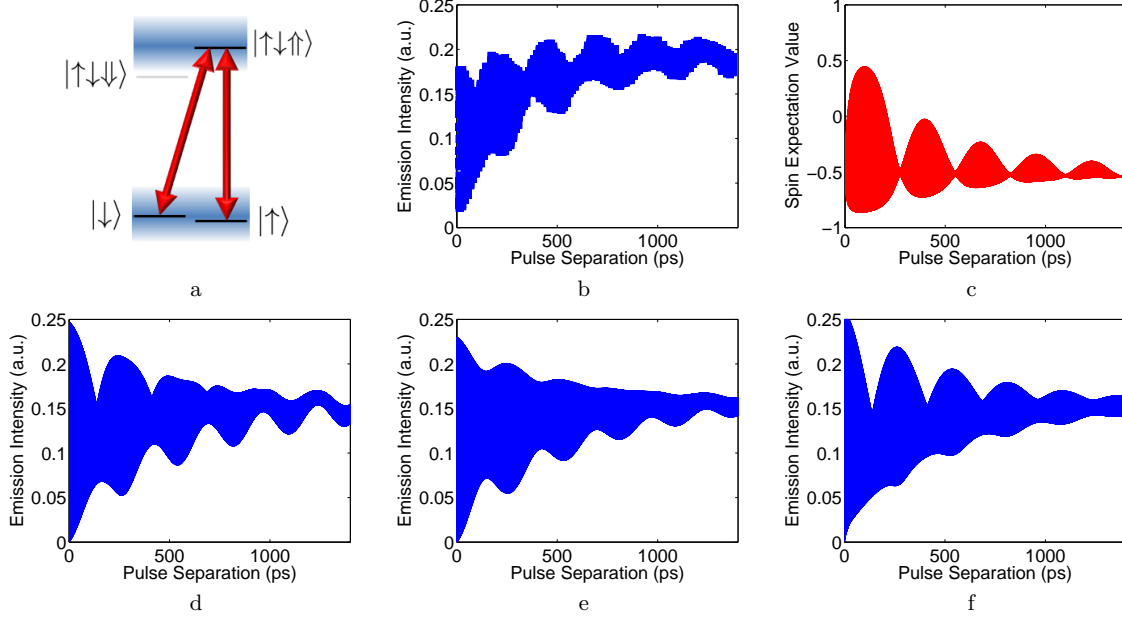


FIG. 4: **a)** Setting the energy detuning of the excitation laser to excite a single vertical transition results in 3-level system behaviour. **b)** The measured emission intensity of the three level system as a function of pulse separation. (The graph appears to be a solid block of colour due to the fast oscillations in X^- intensity with pulse separation. The same is true of the simulated graphs in panels c-f.) **c)** The expectation value of the ground state electron spin in the long time limit as a function of pulse separation. **d)** A full simulation of the expected emission intensity as a function of pulse separation. **e)** The same simulation as panel d), but here the effect of the pulse separation-dependent spin preparation is neglected. Note that this results in a lower beat visibility than the experimental data, indicating that the prepared spin state plays an important role in the expected emission intensity. **f)** The same simulation as panel d) but here the coherence terms between the two electron ground states are rapidly destroyed. This removes the slow oscillatory behavior at late times, indicating that the slow oscillation is a consequence of the preparation of a coherent superposition of the electron ground states.

Setting the laser wavelength degenerate with one of the observed transitions in Fig. 3c, we repeat the RI measurement. We again observe a slow beating pattern with high visibility. This time, the beat frequency corresponds to the energy of the electron Zeeman splitting. A field-dependent measurement allows us to determine the electron g -factor ($|g_e| = 0.58 \pm 0.08$) - in good agreement with $|g_e| = 0.60 \pm 0.05$ made using the standard spectral method [15].

It is surprising that the ground state splitting can cause high visibility beats in the interferogram (Figure 4b). The ground state splitting is rather small so the laser spectrum overlaps with both transitions, as shown in Fig. 4a. Although, in an ideal dot the diagonal transition in Figure 4a is forbidden, heavy-light hole mixing results in a weakly allowed diagonal transition [16–18]. However, we would expect only a low visibility beat if this effect were resulting from a similar mechanism to what is seen in Fig. 3, namely the independent oscillation of populations shared between vertical and diagonal transitions, because of the difference in transition strengths.

This high beat visibility can be explained by the dependence of the state of the electron on the pulse separation. The system is more likely to be excited when the electron is in the $|\uparrow\rangle$ state due to the stronger coupling of the vertical transition to laser field. Therefore, in order to model the 3-level system we must calculate the expected initial state of the electron.

We find that the expected initial state of the electron is dependent on the pulse separation (Figure 4c). This dependence can be intuitively understood by considering weak pulses using a model with two Bloch vectors (note that this explanation neglects any coupling between the two low energy states via the excited state). After the first pulse, the Bloch vectors for the two transitions precess about the z-axis at different rates. When they are completely out of phase the second pulse can then destructively interfere with one transition and constructively interfere with the other. The result is as if we were preferentially driving the constructively interfering transition and only weakly driving the destructively interfering one. After many 2-pulse repetitions, we see spin state preparation as one spin state is being preferentially driven into the excited state. This explains why the nodes in fringe visibility (Figure 4d) correspond to anti-nodes in the spin-expectation value graph (Figure 4c). Including the spin preparation effect in the simulations allows us to recover the surprisingly high beat visibility, (Figure 4d). In contrast, Figure (4e) is the result of ignoring the spin preparation - note the considerably lower beat visibility.

As would be expected, at longer pulse separations this interference has less of an effect and the expected spin-state becomes closer to the calculated value for single pulses.

Next we turn our attention to the slow oscillation in the average emission rate visible in the interferogram, a feature which is particularly noticeable at 600-1400 ps (Figure 4b). This behavior is not seen in the 2 or 4-level systems. The oscillation frequency corresponds to the Larmor frequency of the electron. We determine that not only is the expected population

of the electron spin state important for determining the emission intensity, the coherence matters too. The first pulse creates an impure coherent superposition of the electron spin state by coupling the two spin states via the excited state. Our simulations predict the observed slow oscillation and show that the phase of the electron spin before the second pulse affects the emission intensity. To emphasize this point we destroy the electron coherence terms in the model and see that this removes the slow oscillatory behaviour (Figure 4f). The model predicts that the visibility of these oscillations will be higher at higher pulse powers and this is observed in our measurements (not shown here). The simulations also show that the decay of these oscillations at long times is only dependent on the decay and dephasing times of the electron spin.

Our study of RI in the 3-level system demonstrates that we can prepare a spin by controlling the phase difference between successive pulses. This shows that it is possible to use a single pulsed laser for both spin state preparation and exciton creation, in contrast to work such as [19] which makes use of multiple lasers to address the spin and exciton qubits separately. Measurements of the slow oscillation visible in Fig. 4b at longer delay times should allow direct measurement of the electron spin coherence time. The results also show that it is possible to manipulate the state of the system by coherently driving the forbidden diagonal transitions of a QD in the Faraday geometry with a resonant laser pulse. Finally, we note that the ability to prepare and coherently manipulate an electron spin state, along with the ability to collect output light of all frequencies are key capabilities required to generate electron spin-photon frequency entanglement [20].

Acknowledgments

The authors acknowledge funding from the EPSRC for MBE system used in the production of the QD-LED. J. L. gratefully acknowledges financial support from the EPSRC CDT in Photonic Systems Development and Toshiba Research Europe Ltd.

-
- [1] L. Essen and J. Parry, *Nature* **176**, 280 (1955).
 - [2] S. Haroche and J. M. Raimond, *Exploring the quantum* (Oxford Univ. Press, 2006).
 - [3] A. Ramsay, *Semicond. Sci. Technol.* **25**, 103001 (2010).

- [4] H. Jayakumar, A. Predojević, T. Huber, T. Kauten, G. S. Solomon, and G. Weihs, Phys. Rev. Lett. **110**, 135505 (2013).
- [5] K. Litvinenko, E. Bowyer, P. Greenland, N. Stavrias, J. Li, R. Gwilliam, B. Villis, G. Matmon, M. Pang, B. Redlich, *et al.*, Nat. Commun. **6** (2015).
- [6] G. De Lange, Z. Wang, D. Riste, V. Dobrovitski, and R. Hanson, Science **330**, 60 (2010).
- [7] N. H. Bonadeo, J. Erland, D. Gammon, D. Park, D. Katzer, and D. Steel, Science **282**, 1473 (1998).
- [8] S. Stuffer, P. Ester, A. Zrenner, and M. Bichler, Phys. Rev. Lett. **96**, 037402 (2006).
- [9] Y.-M. He, Y. He, Y.-J. Wei, D. Wu, M. Atatüre, C. Schneider, S. Höfling, M. Kamp, C.-Y. Lu, and J.-W. Pan, Nature Nanotech. **8**, 213 (2013).
- [10] J. Johansson, P. Nation, and F. Nori, Comput. Phys. Commun. **184**, 1234 (2013).
- [11] R. Melet, V. Voliotis, A. Enderlin, D. Roditchev, X. Wang, T. Guillet, and R. Grousson, Phys. Rev. Lett. B **78**, 073301 (2008).
- [12] E. Flagg, A. Muller, J. Robertson, S. Founta, D. Deppe, M. Xiao, W. Ma, G. Salamo, and C.-K. Shih, Nature Phys. **5**, 203 (2009).
- [13] A. Ramsay, A. V. Gopal, E. Gauger, A. Nazir, B. W. Lovett, A. Fox, and M. Skolnick, Phys. Rev. Lett. **104**, 017402 (2010).
- [14] E. Skantzakis, P. Tzallas, J. Kruse, C. Kalpouzos, O. Faucher, G. D. Tsakiris, and D. Charalambidis, Phys. Rev. Lett. **105**, 043902 (2010).
- [15] A. Tartakovskii, T. Wright, A. Russell, V. Fal’Ko, A. Van’kov, J. Skiba-Szymanska, I. Drouzas, R. Kolodka, M. Skolnick, P. Fry, *et al.*, Phys. Rev. Lett. **98**, 026806 (2007).
- [16] A. Delteil, W.-b. Gao, P. Fallahi, J. Miguel-Sanchez, and A. Imamoglu, Phys. Rev. Lett. **112**, 116802 (2014).
- [17] A. V. Koudinov, I. A. Akimov, Y. G. Kusrayev, and F. Henneberger, Phys. Rev. B **70**, 241305 (2004).
- [18] T. Belhadj, T. Amand, A. Kunold, C.-M. Simon, T. Kuroda, M. Abbarchi, T. Mano, K. Sakoda, S. Kunz, X. Marie, and B. Urbaszek, Applied Physics Letters **97**, 051111 (2010).
- [19] D. Press, T. D. Ladd, B. Zhang, and Y. Yamamoto, Nature **456**, 218 (2008).
- [20] W. B. Gao, P. Fallahi, E. Togan, J. Miguel-Sanchez, and A. Imamoglu, Nature **491**, 426 (2012).